TOXICOLOGICAL SCIENCES **78,** 287–294 (2004)
DOI: 10.1093/toxsci/kfh077
Advance Access publication February 19, 2004

Single Cell Analysis of Switch-Like Induction of CYP1A1 in Liver Cell Lines

Carolyn J. Broccardo, Ruth E. Billings, Laura S. Chubb, Melvin E. Andersen,[1] and William H. Hanneman[2]

Department of Environmental and Radiological Health Sciences, Colorado State University, Fort Collins, Colorado 80523-1680

Received October 23, 2003; accepted January 20, 2004

The shape of the dose-response curve may vary depending on whether one examines response at a population or a single cell level. Populations of cells may exhibit a graded response whereas single cell responses may have threshold or switch-like behavior. Studies *in vivo* and *in vitro* using primary hepatocyte cultures have shown that induction of CYP1A1 in the liver exhibits switch-like behavior in response to PCB 126 (3,3′,4,4′,5-pentachlorobiphenyl). The goal of the present study was to determine if two liver cell lines (H4IIE rat hepatoma and Hepa 1c1c7 mouse hepatoma) also show switch-like behavior and develop experimental models for studying mechanisms of these switch-like responses. Both cell lines were analyzed via concentration-response and time-course studies using quantitative real-time PCR, revealing a sigmoidal concentration-response curve for CYP1A1 mRNA induction at the population level. To study CYP1A1 protein induction on a single cell level, flow cytometry was employed. In both cell lines the distribution of fluorescence increased with increasing concentrations of PCB 126. The switch behavior was more pronounced in the H4IIE cells than in the Hepa 1c1c7 cells, exhibiting a well-defined shift of induction from the "off" to the "on" state. The concentration-response curve at the single cell level appeared more switch-like with two populations of cells—basal levels and maximally induced. Immunocytochemistry studies of individual cells also support these conclusions. Our data support the hypothesis that PCB 126 induces CYP1A1 in a switch-like fashion in H4IIE rat hepatoma cells. These cells can now be used to study the mechanism of the biological switch.

Key Words: **PCB; CYP1A1; switch; flow cytometry; H4IIE; Hepa 1c1c7.**

Gene expression may exhibit either a graded or a "switch-like" response to a stimulus (Louis and Becskei, 2002). Single cell studies have further revealed that many enhancer linked genes are generally "on" or "off" in individual cells; the active enhancer increases the probability that the gene will be active in a given cell (Fiering *et al.*, 2000). However, given identical stimuli, some cells will still remain in the "off" state in such a stochastic model of enhancer-gene interaction. Other factors that may contribute to this switch-like, binary response include protein kinase cascades (Ferrell, 1996; Ferrell and Machleder, 1998), transcriptional synergy between transcription factors and promoter elements (Carey, 1998), the interactions of repressors, activators, and co-activators (Blankenship and Matsumura, 1997; Gradin *et al.*, 1999; Mimura *et al.*, 1999), and chromatin remodeling (Okino and Whitlock, 1995). Switch-like behavior of gene induction could explain the observed threshold response of a cell to a particular chemical, and perhaps the phenomenon that some cells appear to be nonresponders, even at the highest concentration.

The shape of the dose-response curve may vary depending on whether one examines response for a population of cells or for individual cells. A population of cells may exhibit a graded response whereas on a single cell basis the response appears threshold or switch-like (Ferrell and Machleder, 1998). Studies of gene induction at the level of individual cells and of the processes that lead to different sensitivities of cells to induction are required to develop improved low dose extrapolations for switch-like or so-called binary responses of cells.

Cytochrome P450 proteins are a superfamily of enzymes involved in the biotransformation of various drugs, carcinogens, and steroid hormones (Estabrook, 1996). CYP1A1 is the classic biomarker of exposure to halogenated aromatic hydrocarbons (HAHs), including 2,3,7,8-tetrachlorodibenzo-*p*-dioxin (TCDD), and the most potent polychlorinated biphenyl agonist, PCB 126 (Hestermann *et al.*, 2000). CYP1A1 is part of the aryl hydrocarbon receptor (AhR) gene battery (Nebert *et al.*, 2000). AhR is a cytosolic receptor that, upon ligand binding, translocates into the nucleus and dimerizes with the aryl hydrocarbon nuclear translocator (Arnt) (Ma, 2001). The ligand-bound AhR-Arnt complex binds to dioxin response elements (DREs) located in the enhancer/promoter region of TCDD responsive genes such as CYP1A1. CYP1A1 displays minimal to no constitutive expression and is highly inducible by PCB 126 and TCDD (Whitlock, 1999).

Previous research has demonstrated a distinctly heteroge-

[1] Present address: CIIT-Centers for Health Research, Six Davis Drive, PO Box 12137, Research Triangle Park, NC 27709.

[2] To whom correspondence should be addressed at Department of Environmental and Radiological Health Sciences, Physiology Building (1680) Room 132, 1680 Campus Delivery, Fort Collins, CO 80523-1680. Fax: (970) 491-7569. E-mail: hanneman@colostate.edu.

neous pattern of CYP1A1 enzyme induction within the rat liver (Andersen *et al.*, 1995; Bars and Elcombe, 1991; Tritscher *et al.*, 1992). Immunohistochemical staining following *in vivo* treatment with TCDD demonstrates that low doses induce CYP1A1 solely within the centrilobular region and as the dose increases the proportion of induced cells increases and staining spreads out toward periportal areas. Within the induced liver, there is a clear boundary between responsive regions (Bars and Elcombe, 1991; Bars *et al.*, 1989). Hence individual hepatocytes appear as either uninduced or fully induced at any specific concentration of TCDD. In our laboratory, primary rat hepatocyte cultures display similar behavior (French *et al.*, in press). On a single cell basis, adjacent cells appear induced/uninduced for CYP1A1 protein and mRNA after *in vitro* PCB 126 treatment as seen by *in situ* hybridization and immunocytochemistry. The concentration-dependent switching response was accompanied by an increase in the proportion of cells within the induced pool; however a single, maximal induction peak did not result. Instead, groups of induced cells exhibited varying degrees of induction intensity. Overall, the resulting distributions appear to support a hybrid switch response, where a switch works in concert with a rheostat, much like a dimmer on a light switch in a home.

The research described here extends the primary rat hepatocyte model by focusing on two liver cell lines, the H4IIE rat hepatoma, and the Hepa 1c1c7 mouse hepatoma cells. The H4IIE cells display switch-like behavior, as previously noted in the *in vivo* and *in vitro* liver cell models. Using flow cytometry to study single cell CYP1A1 protein induction, cells appear either "on" or "off." Studies using small concentration increments to better elucidate the shape of the concentration-response curve and the apparent switch support this hypothesis. As concentration increases, the number of cells expressing CYP1A1 protein increases to the same maximal level of induction, with some cells still not responding, even at the highest concentrations.

MATERIALS AND METHODS

Culture of cell lines. All cell culture products were obtained from Gibco unless otherwise noted. Rat hepatoma H4IIE cells (ATCC) were cultured in DMEM supplemented with 10% FBS and 100 units/ml penicillin/100 μg/ml streptomycin and maintained at 37°C and 5% CO_2. Mouse hepatoma Hepa 1c1c7 cells (ATCC) were cultured in α-MEM without nucleosides supplemented with 10% FBS, 100 units/ml penicillin/100 μg/ml streptomycin and maintained at 37°C and 5% CO_2. For PCR and flow cytometry both cell lines were seeded at 1×10^6 cells/mL in 60 mm culture dishes (Falcon).

PCB 126 treatment. PCB 126 (3,3′,4,4′,5-pentachlorobiphenyl) was obtained from Accustandard (New Haven, CT) and confirmed by GCMS to be pure and free of other congeners. For treatment, PCB 126 was dissolved in DMSO; treatments contained less than 0.25% DMSO. No changes in growth rate or morphology were observed after treatment with DMSO or PCB as compared to naïve cells.

RNA isolation and cDNA synthesis. RNA was isolated using the RNeasy mini kit (Qiagen, Valencia, CA). Briefly, lysis buffer was added to each 60 mm dish and cells were removed using a rubber policeman. The lysate was then homogenized in a QIAshredder spin column and then applied to the RNeasy mini column. The membrane bound RNA was then put through a series of washes and eluted in DEPC water. RNA was quantified on a spectrophotometer and purity was verified on a 1% agarose gel. One μg of total RNA was reverse transcribed using the Promega (Madison, WI) Reverse Transcription system containing oligo $d(T)_{15}$ primers (0.5 μg), AMV reverse transcriptase (15 units), dNTP mix (1 mM each), first strand buffer (10 mM Tris-HCl, 50 mM KCl, 0.1% Triton X-100), $MgCl_2$ (5 mM), and recombinant Rnasin ribonuclease inhibitor (0.5 units) in a final reaction volume of 20 μl. The reaction was performed at 42°C for 15 min and then incubated at 99°C for 5 min to inactivate the reverse transcriptase.

Real-time quantitative RT-PCR. Quantitative PCR was performed in the Bio RAD iCycler iQ Real-Time Detection System. Dr. Nigel Walker (NIEHS) kindly provided the primer and Taqman probe sequences in Table 1. All primer sequences have homology to both the rat and mouse as determined by a BLAST search. The cDNA (50 ng) was amplified in a mixture of 1 mM dNTPs (Invitrogen, Carlsbad, CA), 0.5 μM each of forward and reverse primers (Invitrogen), 0.2 μM Taqman probe primers, 1X PCR buffer F (Invitrogen), and 1 unit Platinum Taq polymerase (Invitrogen) in a 50 μl total reaction. The fluorescent moieties of the Taqman probe primers were 5′ 6-FAM and 3′ Black Hole Quencher-1 (Integrated DNA Technologies Inc., Coralville, IA) Conditions of the PCR were 3 min at 95°C followed by 50 cycles of two-step PCR for 15 s at 95°C and 1 min at 55°C. Each sample was performed in duplicate. The data were normalized by subtracting the difference of the C_T values between the CYP1A1 gene of interest and the β-actin housekeeping gene. This calculation of (CYP1A1 C_T) – (β-actin C_T) is ΔC_T. Fold induction (relative expression) was calculated as $2^{-(S\Delta C_T - C\Delta C_T)}$ where $S\Delta C_T - C\Delta C_T$ is the difference between the sample ΔC_T (PCB 126 treated) and the control ΔC_T (DMSO, untreated). Both the CYP1A1 and β-actin reactions approached 100% efficiency as determined by standard curves. The PCR products were analyzed on agarose gels and found to produce single products.

Flow cytometry. After treatment, cells were trypsinized and washed once in PBS. Cells were resuspended in 2% formaldehyde, EM grade, without methanol (Polysciences, Warrington, PA) and fixed on ice for 30 min. Cells were washed twice in PBS/1% BSA and then permeabilized for 10 min in 0.8% saponin (Sigma, St. Louis, MO) in PBS/1% BSA. Cells were washed once in PBS/1% BSA and blocked for 15 min in 5% goat serum (Sigma) in PBS/1% BSA. Cells were washed once in PBS/1% BSA and incubated with rabbit anti-rat CYP1A1 polyclonal antibody (1:500 dilution, Chemicon) in PBS/1% BSA, 0.8% saponin for 60 min. Cells were washed three times in PBS/1% BSA and incubated with Alexa Fluor 488 goat anti-rabbit IgG (1:200 dilution,

TABLE 1
Primer Sequences Used in Real Time RT-PCR

Gene	Forward primer	Reverse primer	Taqman probe
CYP1A1	5′-tcaaagagcactacaggacatttg	5′-gggttggttaccaggtacatgag	5′-aagggccacatccgggacatca
β-actin	5′-gacaggatgcagaaggagattactg	5′-gctgatccacatctgctggaa	5′-atcaagatcattgctcctcctgag

Note. Primer sequences kindly provided by Dr. Nigel Walker (NIEHS).

Molecular Probes) in PBS/1% BSA, 0.8% saponin for 30 min in the dark. Cells were washed three times in PBS/1% BSA and resuspended in 1 ml PBS and analyzed on the Beckman Coulter EPICS 5 Flow Cytometer. Alexa Fluor 488 was excited by the 488 nm line of an argon ion laser operating at 200 mW of power. Fluorescence was detected by a photomultiplier equipped with a 525 band pass filter. Light scatter was collected in both the forward and right angle directions. Data were processed and displayed on the Cyclops software (Dako Cytomation). To assess nonspecific binding of the antibodies, DMSO and PCB 126 treated samples were incubated with rabbit IgG (Sigma) instead of the rabbit anti-rat CYP1A1 primary antibody. A PCB 126 sample was also incubated with no primary antibody (vehicle only) and then with Alexa 488 to assess any nonspecific binding of the secondary antibody.

Immunocytochemistry (ICC). Cells were seeded on permanox 2-well chamber slides (Nunc, Rochester, NY) at 140,000 cells/well. Cells fixed on slides were stained through immunocytochemistry to visualize CYP1A1 protein levels in individual cells. ICC was performed on duplicate slides for each treatment group. On the day of staining, slides were rehydrated and incubated in 0.3% hydrogen peroxide to quench exogenous peroxidase activity. Slides were immersed in Citra Antigen Retrieval Solution (Biogenex, San Ramon, CA) and microwaved until boiling (approximately 3 min). They were then microwaved another 10 min at low power and allowed to cool. After a 5-min wash in running deionized water, the slides were incubated in PBS with Avidin blocking solution (Vector Labs, Burlingame, CA) at 37°C for 15 min followed by a rinsing off with PBS and incubation with Biotin blocking solution (Vector Labs, Burlingame, CA) for 15 minutes at 37°C. After another quick wash, slides were incubated for 10 min with normal goat serum from Vectastain Avidin-Biotin Complex (ABC) kit (Vector Labs). Without washing, rabbit anti-rat CYP1A1 antibody (Chemicon, Temecula, CA) was added at 1:500 dilution for 15 minutes at 37°C. After a 5-min wash in PBS, biotinylated anti-rabbit IgG antibody was added (Vectastain kit) for 25 min. Slides were washed for 5 min in PBS and ABC reagent (Vectastain kit) was added for 30 min. Following another 5-min wash in PBS, 3-amino-9-ethylcarbazole (AEC; Biomeda) was prepared and added for approximately 5 min at 37°C, then washed off with deionized water. The slides were then counterstained for 30 s with Gill's hematoxylin and washed in running tap water for 10 min. Slides were cover-slipped using water based (Kaiser's) mounting media.

Statistical methods: Real time PCR. Fold induction of the real-time PCR data were calculated using the $2^{-\Delta\Delta CT}$ method (Livak and Schmittgen, 2001). This method normalizes using the housekeeping gene of choice and determines fold induction of a gene due to a chemical treatment. Concentration-response and time-course curves were generated using GraphPad Prism® 3.0. These data were fit based on the Hill relationship:

$$\text{Induction} = \text{Induction}_{max} * \text{Concentration}^n/(\text{Concentration}^n + K_d{}^n),$$

where n is the Hill coefficient and K_d is ligand receptor binding affinity.

The actual transformed equation applied was

$$R(d,t) = R_0 + (R_{max,t} - R_0)/(1 + 10\hat{}\ (\text{LogEC}_{50} - \text{LogDose}) * n^H))$$

where R(d,t) = response at a given time t after dosing; R_0 = initial response; $R_{max,t}$ = maximal response at a given time t after dosing; LogEC_{50} = log dose at 50 percent maximal response; n^H = Hill slope.

This is a sigmoidal dose-response (variable slope) equation that generates a n^H (Hill slope), EC_{50} and r^2 for the concentration-response studies. Each point on the curve represents duplicate experiments. For the time course study, a nonlinear regression (sigmoidal dose-response, identical to the formula above minus the Hill coefficient) was used for the H4IIE cells. R_0, R_{max}, and Log EC_{50} were held constant. Linear regression was used for the Hepa 1c1c7 cells for the time course study.

Flow cytometry. The histograms directly from the flow cytometer were generated in Cyclops (Dako Cytomation, Fort Collins, CO). Statistical analyses were performed using GraphPad® Prism 3.0 and curves were fit using the same sigmoidal dose-response (variable slope) curve fit algorithm as for PCR. Differences between treatments were evaluated using ANOVA and Tukey's Multiple Comparison test ($p < 0.05$).

RESULTS

Real Time RT-PCR

Real time RT-PCR was performed in order to compare previously determined CYP1A1 induction levels in primary rat hepatocytes to the H4IIE rat hepatoma and Hepa 1c1c7 mouse hepatoma cell lines. Both concentration-response and time-course analyses were performed on the two cell lines. H4IIE cells display approximately 1000-fold induction of CYP1A1 at 24 h (Fig. 1a). Induction shifted to maximal between 2.5×10^{-11} to 2.5×10^{-9} M PCB 126 ($EC_{50} = 1.6 \times 10^{-10}$ M, $r^2 = .99$) on this semi-log plot. The time course analysis, at a concentration of 2.5×10^{-8} M, revealed that induction was maximal by 16 h, rising to 2000-fold induction, and down to 1000-fold induction by 48 h (Fig. 1b). The Hepa 1c1c7 cells displayed approximately 30-fold induction of CYP1A1 by 24 h with induction shifting to maximal between 2.5×10^{-11} to 2.5

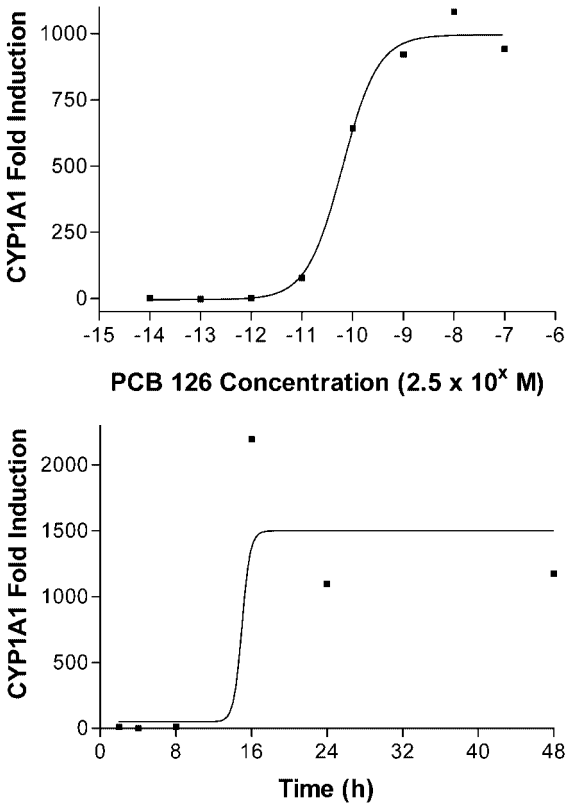

FIG. 1. CYP1A1 mRNA fold induction levels in H4IIE cells. Relative quantification of the mRNA induction levels was accomplished by real time RT-PCR using primers specific for the gene of interest, CYP1A1, and a housekeeping gene, β-actin. (a) 24 h treatment with PCB 126 with concentrations ranged 10-fold from 2.5×10^{-14} to 2.5×10^{-7} M, (b) treatment with 2.5×10^{-8} M PCB 126 for 2, 4, 8, 16, 24, 48 h.

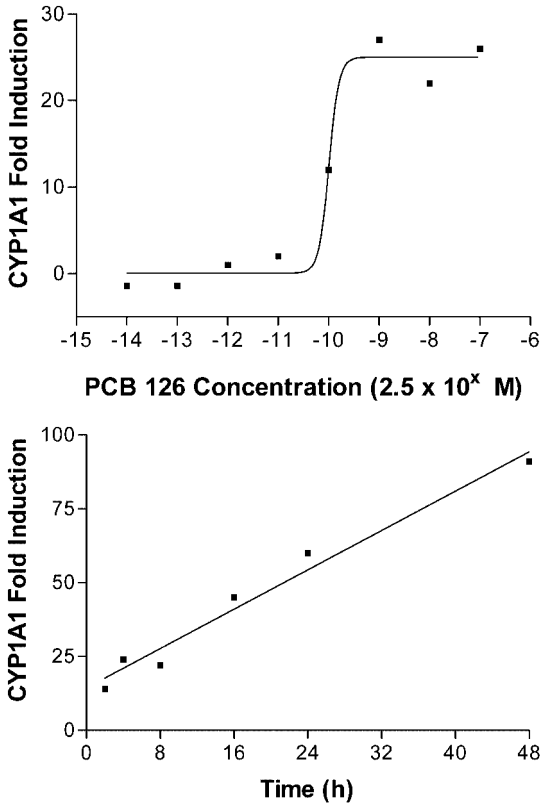

FIG. 2. CYP1A1 mRNA fold induction levels in Hepa 1c1c7 cells. Relative quantification of the mRNA induction levels was accomplished by real time RT-PCR using primers specific for the gene of interest, CYP1A1, and a housekeeping gene, β-actin. (a) 24 h treatment with PCB 126 with concentrations ranged 10-fold from 2.5×10^{-14} to 2.5×10^{-7} M, (b) treatment with 2.5×10^{-8} M PCB 126 for 2, 4, 8, 16, 24, 48 h.

$\times 10^{-9}$ M PCB 126 ($EC_{50} = 2.5 \times 10^{-10}$ M, $r^2 = .98$; Fig. 2a). The time-course analysis, at a concentration of 2.5×10^{-8} M, revealed approximately 100-fold induction of CYP1A1 by 48 h (Fig. 2b) and the level of induction was still increasing. It was determined that the Hill slope for these curves were not reliable due to minimal data points around the midpoint of the curve.

Immunocytochemistry

Immunocytochemistry was performed in order to visually localize CYP1A1 protein on an individual cell basis. The pattern of CYP1A1 staining in H4IIE cells reveal, at a representative maximal concentration of 2.5×10^{-9} M PCB 126 for 24 h, some cells intensely stained for CYP1A1 adjacent to cells that display little to no CYP1A1 staining (Fig. 3b) as compared to DMSO vehicle control (Fig. 3a), which is negative for CYP1A1. A similar pattern can be observed in the Hepa 1c1c7 cells at the same concentration, 2.5×10^{-9} M, for 24 h (Fig. 3d) as compared to DMSO (Fig. 3c). Deciphering a clear pattern of CYP1A1 expression across the population is not entirely possible. Once a cell is on there are several patterns

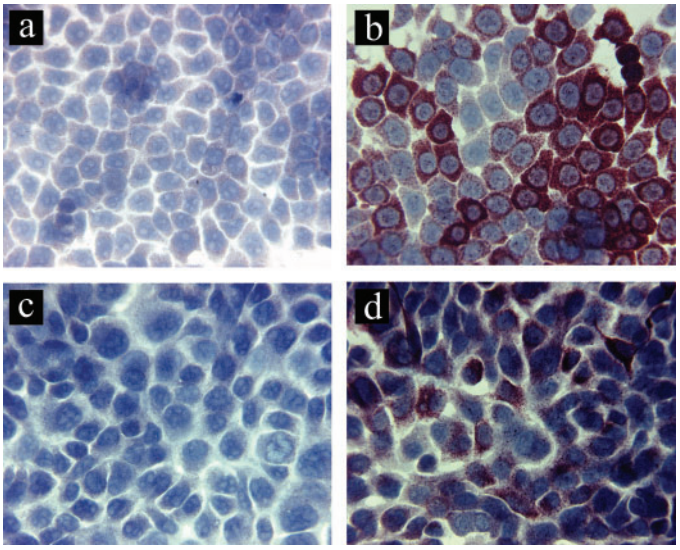

FIG. 3. Immunocytochemistry stained slides reflecting the distribution of induced CYP1A1 protein within cells after 24 h. The Gill's hematoxylin counterstained photomicrographs are under 40X magnification. (a) H4IIE cells, DMSO, (b) H4IIE cells, 2.5×10^{-9} M, (c) Hepa 1c1c7 cells, DMSO, (d) Hepa 1c1c7 cells, 2.5×10^{-9} M.

seen. Many neighboring cells may be on, but there are also neighboring cells with far less expression or cells that are off. Further, completely isolated cells, i.e., cells with no direct contact with other cells, may be on or off. As such, it is not possible to say that CYP1A1 expression occurs in definitive "clusters."

Flow Cytometry

Flow cytometry was used to measure CYP1A1 protein levels after PCB 126 treatments in H4IIE and Hepa 1c1c7 cell lines. Within the histograms (Figs. 4 and 5) region 1 is gated to include the background fluorescence of the DMSO vehicle

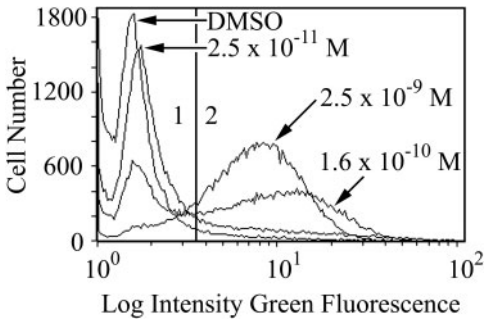

FIG. 4. CYP1A1 protein induction in H4IIE cells. This histogram overlay of several concentrations from Figure 7 shows the pattern of induction on a single cell basis within a concentration, and between concentrations of PCB 126. The populations of induced cells express similar levels of CYP1A1 as seen by the overlap of the curves, with the number of induced cells increasing with concentration of PCB 126.

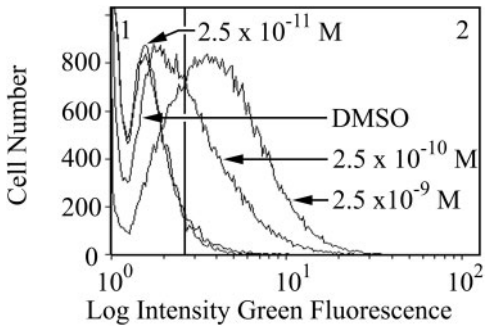

FIG. 5. CYP1A1 protein induction in Hepa 1c1c7 cells. This histogram overlay of several concentrations from Figure 9 shows the pattern of induction on a single cell basis within a concentration, and between concentrations of PCB 126. The populations of induced cells express similar levels of CYP1A1 as seen by the overlap of the curves, with the number of induced cells increasing with concentration of PCB 126.

control; cells within region 2 show an increase in green fluorescence representing CYP1A1 expression. There is a concomitant increase in cells in region 2 as concentration increases, representing more cells expressing CYP1A1 on a single cell basis. The increase in the number of cells expressing CYP1A1 is marked between 1.6×10^{-10} to 2.5×10^{-9} M in the H4IIE cells (Fig. 4), and between 2.5×10^{-10} to 2.5×10^{-9} M in the Hepa 1c1c7 cells (Fig. 5) with the population of induced cells expressing similar levels of CYP1A1 as seen by the overlap of the curves. The concentration of 2.5×10^{-13} M has a nearly identical curve to that of the DMSO control in both cell lines. Rabbit IgG isotype controls and secondary antibody only controls had minimal to no fluorescence, as compared to the DMSO curves in all experiments. Single cell flow cytometry concentration-response analysis of H4IIE cells is shown in Figure 6. A concentration-response ranging from 2.5×10^{-13} M to 2.5×10^{-5} M revealed maximal induction of CYP1A1 by 2.5×10^{-10} M with approximately 80% of the cell population responding. The concentrations of 2.5×10^{-13} to 2.5×10^{-11} are not statistically significant from DMSO ($p < 0.05$). To better define the shape of the H4IIE concentration-response curve smaller concentration increments were used as seen in Figure 7. The incremental doses used were: 1.6×10^{-9}, 10×10^{-10}, 6.3×10^{-10}, 4×10^{-10}, 2.5×10^{-10}, 1.6×10^{-10}, 10×10^{-11}, 6.3×10^{-11}, and 4×10^{-11} M PCB 126. These are equally spaced doses between 2.5×10^{-9} and 2.5×10^{-11} M on a log scale. Triplicate experiments were performed using the dose increments, and these data were combined with the original dose response curve (Fig. 6) to create Figure 7. The $r^2 = .93$, $EC_{50} = 7.2 \times 10^{-11}$ M, and $n^H = 1.3$. Identical experiments were performed with the Hepa 1c1c7 cells, as seen in Figures 8 and 9. Maximal induction of CYP1A1 was obtained by 2.5×10^{-9} M, with approximately 70% of the cell population responding (Fig. 8). The concentrations of 2.5×10^{-13} to 2.5×10^{-11} were not statistically significant from DMSO ($p < 0.05$). Incremental concentrations yielded an $r^2 = .96$, $EC_{50} = 2.13 \times 10^{-10}$ M, and $n^H = 1.8$ (Fig. 9).

DISCUSSION

This research demonstrates that the H4IIE rat hepatoma cell line also demonstrates a threshold, switch-like response at the single cell level to the CYP1A1 inducer, PCB 126. This behavior agrees with previous research from our laboratory, supporting a switch model of CYP1A1 induction in primary rat hepatocytes as seen using *in situ* hybridization (French *et al.*, in

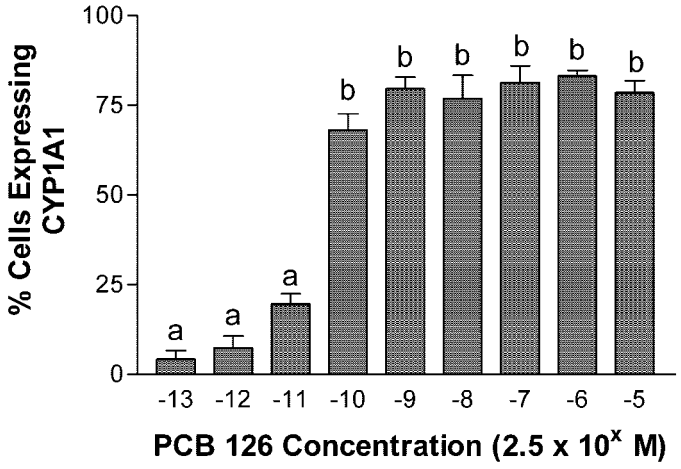

FIG. 6. CYP1A1 protein induction in H4IIE cells following a 24 h PCB 126 treatment using concentrations ranging 10-fold from 2.5×10^{-13} to 2.5×10^{-5} M as measured with flow cytometry. The concentrations 2.5×10^{-13} to $^{-11}$ are not statistically significant from DMSO ($p < 0.05$). Bars represent the ± SEM of at least three independent experiments. Different letters above bars represent significant difference between treatments (a ≠ b), $p < 0.05$.

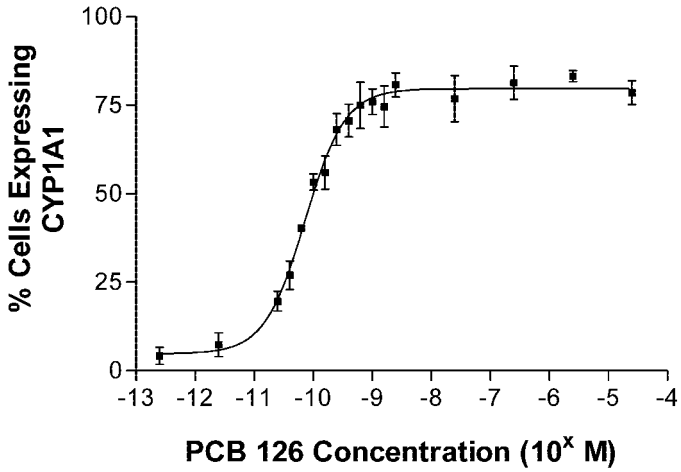

FIG. 7. CYP1A1 protein induction in H4IIE cells following a 24 h PCB 126 treatment. This figure is a combination of the triplicate data from Figure 4 and the addition of eight small dose increments between 2.5×10^{-11} to 2.5×10^{-9} M, performed in triplicate, as measured with flow cytometry. Bars represent the ± SEM of at least three independent experiments.

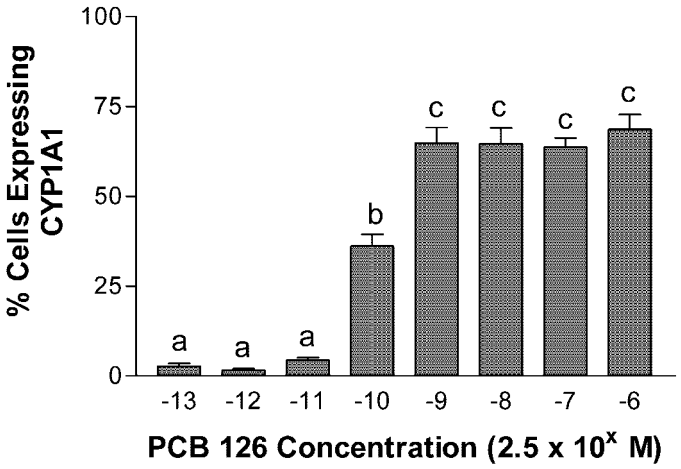

FIG. 8. CYP1A1 protein induction in Hepa 1c1c7 cells following a 24 h PCB 126 treatment using concentrations ranging 10-fold from 2.5×10^{-13} to 2.5×10^{-6} M as measured with flow cytometry. The concentrations 2.5×10^{-13} to $^{-11}$ are not statistically significant from DMSO ($p < 0.05$). Bars represent the ± SEM of at least three independent experiments. Different letters above bars represent significant difference between treatments (a ≠ b ≠ c), $p < 0.05$.

press). Studies *in vivo* also indicated that hepatic CYP1A1 induction was switch-like with characteristics of a hybrid-model (Bars and Elcombe, 1991; Bars *et al.*, 1989). Such a hybrid switch model is comparable to a dimmer on a light switch in a home, where a switch works in concert with a rheostat. Experimentally, such a hybrid switch model on the single cell level represents an initial induction threshold then a graded response thereafter. In the present study, flow cytometry was used to quantify the level of CYP1A1 protein in single cells. It is assumed that CYP1A1 protein levels reflect PCB 126's effects on CYP1A1 gene expression since the correlation of CYP1A1 protein and mRNA is well documented. The correspondence between protein induction and mRNA induction was also examined in the studies with primary hepatocytes (French *et al.*, in press).

Gene induction at the single cell level may display two types of responses: graded (linear) or threshold/switch (binary). The linear curve implies that there is a uniform, cellular response at every concentration; therefore all, cells will display the same level of CYP1A1 induction. With a binary switch, there are some concentrations where there is no response, and then a sharp rise in induction occurs with increasing concentration. As a result, a cell exists in two stable states: uninduced or induced. In reality, however, cellular response may not be as clear cut as the graded or switch theoretical models would define. Cells may, in fact, respond in an intermediate, hybrid fashion. Such a response could be defined as a hybrid switch, whereby cells must pass an initial concentration-threshold, then exhibit a graded response thereafter (Fig. 10).

The H4IIE flow cytometry data presented here support a switch response. In this case, the induced population has a distribution of staining characteristics, but populations still move from a basal state to an induced state in a binary manner. Within one concentration, once a cell is induced it may express varying amounts of CYP1A1 (Figs. 4 and 5). Further, with increasing concentration, the number of CYP1A1 expressing cells increases, with all activated cells displaying the same range in induction as seen by the overlapping curves (in region 2). If the response were graded at the single cell level, a concentration-dependent horizontal shift in curves would be seen, representing a simultaneous shift in all cells with increasing concentration. The data with the Hepa 1c1c7 cells show an increase in CYP1A1 expression with dose, however, provide less resolution between induced and uninduced curves which

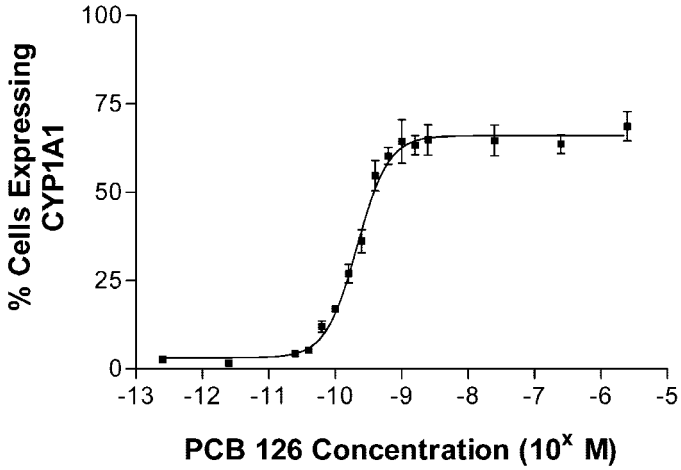

FIG. 9. CYP1A1 protein induction in Hepa 1c1c7 cells following a 24 h PCB 126 treatment. This figure is a combination of the triplicate data from Figure 6 and the addition of eight small dose increments between 2.5×10^{-11} to 2.5×10^{-9} M, performed in triplicate, as measured with flow cytometry. Bars represent the ± SEM of at least three independent experiments.

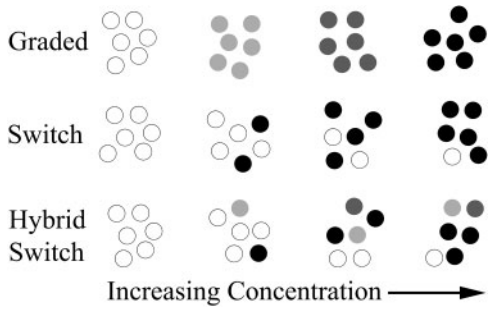

FIG. 10. Three induction models presented on a diagrammatic, cellular level. The graded model has uniform gene induction within one dose, with all cells eventually responding. The switch model displays more and more cells responding in a binary fashion with dose, with some nonresponders even at the highest dose. The hybrid switch model is a combination of the graded and switch models. Once a cell is induced it may display a range of induction levels. There are still nonresponders even at the highest dose.

results in a less definitive conclusion regarding the switch-like nature of this cell line.

The goal of the ICC was to qualitatively show the phenomenon of on and off cells within one dose, and as such was consistent with the flow cytometry data. Cells exposed to a single concentration of PCB 126 displayed a range of induction once they are "on" and can be seen adjacent to uninduced cells (Fig. 3). If the cells responded in a graded, linear fashion, one would expect all of the cells to have a similar level of induction within one concentration. Further, cell cycle does not appear to affect the CYP1A1 protein expression pattern. Cells were serum starved for 48 h, treated with 2.5×10^{-7} M PCB 126, 2.5×10^{-10} M PCB 126, or DMSO for 24 h. The pattern of CYP1A1 protein expression did not change as seen in ICC (data not shown). Both the immunocytochemistry and flow cytometry experiments show that there are some cells in which CYP1A1 is not induced, even at high concentrations of PCB 126. Interestingly, flow cytometry using murine epidermal cells also showed a population of cells that did not respond to β–naphthoflavone in the induction of CYP1A1 (Stauber *et al.*, 1995).

On a population level, the H4IIE and Hepa 1c1c7 cells display a continuous concentration-response curve for CYP1A1 mRNA induction as seen in primary rat hepatocytes (French *et al.*, in press) using quantitative real-time PCR (Figs. 1 and 2). Of note, there appears to be low-level constitutive expression of CYP1A1 mRNA in the Hepa 1c1c7 cells as seen in Figure 2b at time zero. This is not without precedence; Santini *et al.* (2001) also found low-level constitutive expression of CYP1A1 mRNA in DMSO treated Hepa 1c1c7 cells. This might explain the comparatively lesser fold-induction of CYP1A1 mRNA as compared to the H4IIE cells. This low-level constitutive expression is not detectable using ICC or flow cytometry methods that measure protein, perhaps due to the higher sensitivity of quantitative real-time PCR.

How might such a hybrid switch response fit in with the accepted CYP1A1 induction model? AhR is a cytosolic receptor bound to two 90 kDa heat shock protein (hsp90) molecules, an immunophilin-related AIP/XAP/ARA9 protein, and to a p23 chaperone protein. After ligand binding, AhR dissociates from this complex, translocates into the nucleus, and dimerizes with Arnt. The ligand-bound AhR-Arnt complex acts as a transcription factor complex and binds to specific dioxin response elements (DREs) located in the enhancer/promoter region of dioxin responsive genes such as CYP1A1 (Ma, 2001; Whitlock, 1999). However, there are additional modulators in this process that may contribute to the switch response. For example, it is known that the MAPKs (mitogen activated protein kinases), ERK (extracellular regulated kinase), and JNK (c-Jun N-terminal kinase) are activated independently of the AhR (i.e., AhR is not required for their activation), yet are essential for AhR mediated CYP1A1 induction (Tan *et al.*, 2002). Further, the MAPK cascade has the potential to convert a graded stimulus into a switch-like response, through a phenomenon termed ultrasensitivity, whereby multiple events working in concert allow for a rapid activation of a signal transduction cascade (Ferrell, 1996; Goldbeter and Koshland, 1984; Huang and Ferrell, 1996). The concept of ultrasensitivity emphasizes the fact that the slope of the stimulus/response curve is steeper than that of a hyperbolic Michaelis-Menten enzyme. The necessity of the MAPK cascade for CYP1A1 induction introduces the possibility of a MAPK mediated switch acting through a form of ultrasensitivity. In addition, a variety of serine/threonine and/or tyrosine phosphorylation events are now recognized to be crucial to the regulation and activity of the AhR pathway. For example, phosphorylation of AhR positively regulates the DNA binding activity of AhR, and phosphorylation on Arnt is necessary for dimerization between AhR and Arnt (Park *et al.*, 2000). Protein kinase C (PKC) has also been shown to cause a synergistic increase in ligand-induced CYP1A1 gene induction (Chen and Tukey, 1996) and has also been shown to be activated by AhR ligand (Hanneman *et al.*, 1996), perhaps by AhR-independent sustained elevation of intracellular free calcium (Puga *et al.*, 1997). These nongenomic, enzymatic events are additional processes that may contribute to the observed threshold response.

In addition to nongenomic, enzymatic cell-signaling events, the genomic interactions of the AhR-Arnt heterodimer with the DREs may also generate a switch. Conversion of the CYP1A1 gene from a silent phenotype to an accessible target for activation by the heterodimeric transcription complex may require histone modification that could also regulate a switch (Okino and Whitlock, 1995). Whether the switch is genomic or nongenomic, the result would be the same: transcription cannot begin until some critical event occurs in the AhR pathway.

In conclusion, these studies support the hybrid switch model for CYP1A1 induction by PCB 126 in the H4IIE rat hepatoma cells. More critically, even at high concentrations, there are nonresponding cells, indicating some critical event has not transpired in these cells: the so-called switch. Studies to further elucidate the mechanism of the hybrid switch response are currently underway in our laboratory.

ACKNOWLEDGMENTS

This work was supported by CSU College of Veterinary Medicine and Biomedical Sciences, NIEHS Pre-Doctoral Training Grant #ESS07321-01, and by a contract RSK0005 of the American Chemistry Council. We would like to thank Leslie Armstrong and Dr. Michael Fox for their generous help with flow cytometry.

REFERENCES

Andersen, M. E., Mills, J. J., Jirtle, R. L., and Greenlee, W. F. (1995). Negative selection in hepatic tumor promotion in relation to cancer risk assessment. *Toxicology* **102,** 223–237.

Bars, R. G., and Elcombe, C. R. (1991). Dose-dependent acinar induction of cytochromes P450 in rat liver. Evidence for a differential mechanism of

induction of P450IA1 by beta-naphthoflavone and dioxin. *Biochem. J.* **277,** 577–580.

Bars, R. G., Mitchell, A. M., Wolf, C. R., and Elcombe, C. R. (1989). Induction of cytochrome P-450 in cultured rat hepatocytes. The heterogeneous localization of specific isoenzymes using immunocytochemistry. *Biochem. J.* **262,** 151–158.

Blankenship, A., and Matsumura, F. (1997). 2,3,7,8-Tetrachlorodibenzo-p-dioxin-induced activation of a protein tyrosine kinase, pp60src, in murine hepatic cytosol using a cell-free system. *Mol. Pharmacol.* **52,** 667–675.

Carey, M. (1998). The enhanceosome and transcriptional synergy. *Cell* **92,** 5–8.

Chen, Y. H., and Tukey, R. H. (1996). Protein kinase C modulates regulation of the CYP1A1 gene by the aryl hydrocarbon receptor. *J. Biol. Chem.* **271,** 26261–26266.

Estabrook, R. W. (1996). The remarkable P450s: A historical overview of these versatile hemeprotein catalysts. *FASEB J.* **10,** 202–204.

Ferrell, J. E., Jr. (1996). Tripping the switch fantastic: How a protein kinase cascade can convert graded inputs into switch-like outputs. *Trends Biochem. Sci.* **21,** 460–466.

Ferrell, J. E., Jr., and Machleder, E. M. (1998). The biochemical basis of an all-or-none cell fate switch in Xenopus oocytes. *Science* **280,** 895–898.

Fiering, S., Whitelaw, E., and Martin, D. I. (2000). To be or not to be active: The stochastic nature of enhancer action. *Bioessays* **22,** 381–387.

French, C. T., Hanneman, W. H., Chubb, L. S., Billings, R. E., and Andersen, M. E. (in press). Induction of CYP1A1 in primary rat hepatocytes by 3,3′,4,4′,5-pentachlorobiphenyl: Evidence for a switch circuit element. *Toxicol. Sci.* **78,** 276–286.

Goldbeter, A., and Koshland, D. E., Jr. (1984). Ultrasensitivity in biochemical systems controlled by covalent modification. Interplay between zero-order and multistep effects. *J. Biol. Chem.* **259,** 14441–14447.

Gradin, K., Toftgard, R., Poellinger, L., and Berghard, A. (1999). Repression of dioxin signal transduction in fibroblasts. Identification Of a putative repressor associated with Arnt. *J. Biol. Chem.* **274,** 13511–13518.

Hanneman, W. H., Legare, M. E., Barhoumi, R., Burghardt, R. C., Safe, S., and Tiffany-Castiglioni, E. (1996). Stimulation of calcium uptake in cultured rat hippocampal neurons by 2,3,7,8-tetrachlorodibenzo-p-dioxin. *Toxicology* **112,** 19–28.

Hestermann, E. V., Stegeman, J. J., and Hahn, M. E. (2000). Relative contributions of affinity and intrinsic efficacy to aryl hydrocarbon receptor ligand potency. *Toxicol. Appl. Pharmacol.* **168,** 160–172.

Huang, C. Y., and Ferrell, J. E., Jr. (1996). Ultrasensitivity in the mitogen-activated protein kinase cascade. *Proc. Natl. Acad. Sci. U.S.A.* **93,** 10078–10083.

Livak, K. J., and Schmittgen, T. D. (2001). Analysis of relative gene expression data using real-time quantitative PCR and the 2(-Delta Delta C(T)) method. *Methods* **25,** 402–408.

Louis, M., and Becskei, A. (2002). Binary and graded responses in gene networks. *Sci. STKE* **2002,** PE33.

Ma, Q. (2001). Induction of CYP1A1. The AhR/DRE paradigm: Transcription, receptor regulation, and expanding biological roles. *Curr. Drug Metab.* **2,** 149–164.

Mimura, J., Ema, M., Sogawa, K., and Fujii-Kuriyama, Y. (1999). Identification of a novel mechanism of regulation of Ah (dioxin) receptor function. *Genes Dev.* **13,** 20–25.

Nebert, D. W., Roe, A. L., Dieter, M. Z., Solis, W. A., Yang, Y., and Dalton, T. P. (2000). Role of the aromatic hydrocarbon receptor and [Ah] gene battery in the oxidative stress response, cell cycle control, and apoptosis. *Biochem. Pharmacol.* **59,** 65–85.

Okino, S. T., and Whitlock, J. P., Jr. (1995). Dioxin induces localized, graded changes in chromatin structure: implications for Cyp1A1 gene transcription. *Mol. Cell. Biol.* **15,** 3714–3721.

Park, S., Henry, E. C., and Gasiewicz, T. A. (2000). Regulation of DNA binding activity of the ligand-activated aryl hydrocarbon receptor by tyrosine phosphorylation. *Arch. Biochem. Biophys.* **381,** 302–312.

Puga, A., Hoffer, A., Zhou, S., Bohm, J. M., Leikauf, G. D., and Shertzer, H. G. (1997). Sustained increase in intracellular free calcium and activation of cyclooxygenase-2 expression in mouse hepatoma cells treated with dioxin. *Biochem. Pharmacol.* **54,** 1287–1296.

Santini, R. P., Myrand, S., Elferink, C., and Reiners, J. J., Jr. (2001). Regulation of Cyp1a1 induction by dioxin as a function of cell cycle phase. *J. Pharmacol. Exp. Ther.* **299,** 718–728.

Stauber, K. L., Laskin, J. D., Yurkow, E. J., Thomas, P. E., Laskin, D. L., and Conney, A. H. (1995). Flow cytometry reveals subpopulations of murine epidermal cells that are refractory to induction of cytochrome P-4501A1 by beta-naphthoflavone. *J. Pharmacol. Exp. Ther.* **273,** 967–976.

Tan, Z., Chang, X., Puga, A., and Xia, Y. (2002). Activation of mitogen-activated protein kinases (MAPKs) by aromatic hydrocarbons: Role in the regulation of aryl hydrocarbon receptor (AHR) function. *Biochem. Pharmacol.* **64,** 771.

Tritscher, A. M., Goldstein, J. A., Portier, C. J., McCoy, Z., Clark, G. C., and Lucier, G. W. (1992). Dose-response relationships for chronic exposure to 2,3,7,8-tetrachlorodibenzo-p-dioxin in a rat tumor promotion model: Quantification and immunolocalization of CYP1A1 and CYP1A2 in the liver. *Cancer Res.* **52,** 3436–3442.

Whitlock, J. P., Jr. (1999). Induction of cytochrome P4501A1. *Annu. Rev. Pharmacol. Toxicol.* **39,** 103–125.